A NOTE ON DFT FILTERS: CYCLE EXTRACTION AND 'GIBBS' EFFECT CONSIDERATIONS

By

Melvin. J. Hinich
Applied Research Laboratories, University of Texas at Austin,
Austin, TX 78712-1087
Phone: +1 512 232 7270
Email: hinich@austin.utexas.edu

John Foster
School of Economics, University of Queensland,
St Lucia, QLD, 4072, Australia
Phone: +61 7 3365 6780
Email: j.foster@uq.edu.au

and

Phillip Wild*
School of Economics and ACCS, University of Queensland,
St Lucia, QLD, 4072, Australia
Phone: +61 7 3346 9258
Email: p.wild@uq.edu.au

* Address all correspondence to Phillip Wild, School of Economics, University of Queensland, St Lucia, QLD, 4072, Australia; Email:p.wild@uq.edu.au, Phone: +61 7 3346 9258.

ABSTRACT

The purpose of this note is to analyse the capability of bandpass filters to extract a known periodicity. The specific bandpass filters considered are a conventional Discrete Fourier Transform (DFT) filter and the filter recently proposed in Iacobucci-Noullez (2004, 2005). We employ simulation methods to investigate cycle extraction properties. We also examine the implications arising from the Gibbs Effect in practical settings typically confronting applied macroeconomists.

Keywords: business cycles, bandpass filter, cycle extraction, Discrete Fourier Transform (DFT), Gibbs Effect.

1. INTRODUCTION

There has been considerable attention paid to designing various filters to extract business cycle components from macroeconomic time series. In economics, some of the best-known filters are the Hodrick-Prescott (HP) and Baxter-King (BK) filters.[1] In the economics literature less prominence has been given to the design and implementation of frequency domain filters based on DFT methods, including the capacity of the filters to successfully extract cyclical components.

In this note, we investigate whether the filters can extract a known deterministic periodicity while requiring the filter to pass over another periodicity, deliberately designed to fall outside the passband. This is a simple task that we would reasonably expect any filtering algorithm to be able to successfully accomplish.

The above-mentioned deterministic periodic model provides the best methodological framework for demonstrating the key findings we wish to present in this note. However, our results also hold for the more general model of a stationary stochastic periodic process whose innovations are additive Gaussian noise variates, as demonstrated in Hinich, Foster and Wild (2008)a, Section 5.[2]

---

[1] Hodrick and Prescott (1997) and Baxter and King (1999). Also see King and Rebelo (1993), Cogley and Nason (1995), Pedersen (2001) and Murray (2003).

[2] We assume that the data has been appropriately de-trended using an 'appropriate' de-trending method. The filtering operation itself should not to be interpreted as a de-

We also examine the role that the Gibbs Effect might play in practical attempts at business cycle extraction undertaken in an environment familiar to applied macroeconomists – i.e. single realizations of small to moderate length macroeconomic time series data. Such situations are a long way from the mathematical environment that is assumed to underpin theoretical representations of the Gibbs Effect.

In the next section, we outline the role that the DFT plays in designing bandpass filters. We also clarify the role that the Gibbs Effect might be expected to play in practical business cycle extraction exercises. In Section 3, we outline the simulation model. In Section 4, key results from the simulations will be presented. Finally, Section 5 contains concluding comments.

2. DISCRETE FOURIER TRANSFORM AND BANDPASS FILTERS

Suppose the bandpass filter is to be applied to a discrete-time data series $x(t_n)$ (i.e. published macroeconomic time series data) where $t_n = n\tau$, τ is the sampling interval and $x(t_n)$ has finite length $T = N\tau$.[3] In this situation, the appropriate Fourier Transform is the Discrete Fourier Transform (DFT). The DFT maps a sequence of N data points $\{x(0), x(1), \ldots, x(N-1)\}$ in the time domain to a set of N equally spaced

---

trending operation. The filters are to be applied to the transformed data after it has been de-trended.

[3] We can set the first observation index to zero and $\tau = 1$.

amplitudes in the frequency domain at the frequency values $f_k = \frac{k}{T}$ termed Fourier or harmonic frequencies. The (time to frequency) DFT is defined by

$$A_x(k) = \sum_{n=0}^{N-1} x(t_n) \exp(-i2\pi f_k t_n). \quad (1)$$

The highest harmonic frequency index is $[N/2] = N/2$ if N is even and $[N/2] = (N-1)/2$ if N is odd. The Fourier Transform outlined in (1) differs from the 'Discrete-Time Fourier Transform' concept that conventionally underpins analysis of ideal filter response.[4]

The inverse (frequency to time) DFT is

$$x(t_n) = N^{-1} \sum_{k=0}^{N-1} A_x(k) \exp(i2\pi f_k t_n). \quad (2)$$

The complex amplitudes $A_x(k)$ contain all the information about the finite record of the time series. The fundamental limit to resolving amplitudes is T *(or* N*)*, the length of the record whose associated frequency $f_1 = \frac{1}{T}$ is called the fundamental frequency. It is *impossible* to

[4] The main point of difference between (1) and the 'Discrete-Time Fourier Transform' is that the latter involves a doubly infinite summation of filter input $x(t_n)$ [instead of the finite sum in (1)] which produces a continuous frequency response defined over the interval $(-\pi, \pi)$ [instead of the discrete frequency set $\left(0, N/2\right)$ associated with (1)]. The impulse response of the 'Discrete-Time Fourier Transform' for an ideal low pass filter is the 'sinc' function.

exactly compute the true values of $A_x(f)$ for frequencies less than the fundamental frequency and in between the higher harmonic frequencies. Amplitudes whose frequencies are not the Fourier frequencies can only be interpolated with error.

Suppose we wish to analyze the periodic nature of the time series in the passband (f_{k_1}, f_{k_2}). We want to filter out the Fourier amplitudes whose indices are less than k_1 and greater than k_2. This can be accomplished using the FFT by 'zeroing out' all the complex FFT values outside the passband – that is, by utilizing an ideal bandpass filter whose discrete-frequency transfer function is $H(f_k) = 1$ for $k_1 \le k \le k_2$, $-k_2 \le -k \le -k_1$ and zero otherwise. Then the filtered time series is

$$y(t_n) = \frac{1}{N}\left[\sum_{k=k_1}^{k_2} A_x(f_k)\exp(i2\pi f_k t_n) + \sum_{k=N-k_2}^{N-k_1} A_x(f_k)\exp(i2\pi f_k t_n)\right]. \quad (3)$$

The time domain representation of filter coefficients is the inverse Discrete Fourier Transform of the discrete-frequency transfer function. If we set $f_{k_1} = 0$ producing the 'lowpass' version of the ideal filter, the impulse response is the 'Dirichlet' kernel.

In the literature, the 'Discrete-Time Fourier Transform' has been employed instead of the DFT whereas the latter is the appropriate concept for discrete-time finite length time series data. Because of this, the common practice has been to truncate the doubly infinite ideal filter

coefficient sequence retaining only a limited number of its central elements and then convolving this truncated filter with the data to bandpass the series in the time domain. This truncation process generates the Gibbs Effect - an undesirable effect producing a ripple effect whereby the gain of the filter's frequency response fluctuates within both the stopband and passband, producing deviations from the desired ideal frequency response for continuous time filtering [see Papoulis (1962, pp.30-31), Kufner and Kadlec (1971, pp. 225-228), Bracewell (1978, 209-211), Priestley (1981, p.561)].

The leakage effect does not directly apply for the use of the DFT to filter a finite sample of a time series and reflects unavoidable inherent limitations associated with the use of finite length discrete-time data confronting applied macroeconomists. The ideal frequency response can be synthesized at the discrete set of Fourier frequency amplitudes. However, this set of frequency amplitudes is the only frequency concept identifiable when using the DFT outlined in (1)-(2). It is not possible to synthesize a continuous frequency set in the interval $(-\pi,\pi)$. Thus, it is not possible to identify or preserve all components in the (continuous) frequency interval $(-\pi,\pi)$ when applying the DFT to 'real world' macroeconomic data. As a consequence, it is only possible to strictly define 'stopband-passband' cutoffs that coincide with Fourier frequencies and hence, are sub-multiples of both the sample size T and fundamental

frequency f_1. Thus, the only observable frequencies are the Fourier frequencies themselves – the (discrete) set of frequencies at which it is possible to synthesize an ideal frequency response.

To demonstrate the ideal frequency response of the DFT filter, we apply the DFT filter to a unit impulse sequence $\{x(0), x(1), x(2), ..., x(N-1)\}$ = $\{1,0,0,...,0\}$. We adopt a sample size of 120 observations corresponding, for example, to 30 years of quarterly data and define the passband of (24,6) quarters. In terms of frequency (inverted period), the passband is given by (1/24,1/6) = (0.042,0.167).

The frequency response is depicted in Figure 1 and is derived by applying (1) to the unit impulse series and applying the ideal frequency response at the Fourier frequency amplitudes (defined by the 'dot' points in Figure 1). It is evident from inspection of Figure 1 that the ideal frequency response is synthesized at the Fourier frequency amplitudes – i.e. see the 'DFT Filter' response.[5] It should be noted that the curves in Figure 1 are strictly defined only at the discrete Fourier frequencies themselves - it is not a continuous function of frequency.

It is apparent that the 'ripples' associated with the Gibbs Effect are *not observable* – they would lie in the continuum *between* the 'observable' discrete set of Fourier frequency amplitudes. Varying the sample size T

[5] It should be noted that in all figures reported in this note all results associated with the conventional DFT bandpass filter will be labeled 'DFT Filter'.

(and fundamental frequency) by 'zero padding' or dropping data points will not change this basic result.

Figure 1 about here.

The application of the inverse DFT (2) to the discrete ideal frequency response outlined in Figure 1 is documented in Figure 2 – i.e. see the 'DFT Filter' function. This 'function' is symmetrical about N/2, i.e. data point 60 in Figure 2. This function is strictly defined only at the discrete data points represented by the 'dots' in Figure 2 and depicts a discrete finite symmetrical set of (time-domain) filter coefficients. The finite length of this set of filter coefficients means that a truncation process has been automatically imposed on the sequence of filter coefficients.

Figure 2 about here.

In the literature (utilizing the 'Discrete-Time Fourier Transform') window methods have been conventionally applied to minimize the adverse affects of the Gibbs effect (see Priestley (1981, pp.561-562)). This approach has been recently 'revived' in Iacobucci-Noullez (2004, 2005) who proposed the use of a convolved windowed Bandpass DFT Filter Algorithm.[6] This algorithm involves smoothing the '0-1' transition at the 'stopband-passband' cutoffs by using a taper that is linked to specific spectral windows. In this note, we use the 'Hamming' spectral window

[6] It should be noted that in all figures reported in this note all results associated with the Iacobucci-Noullez convolved windowed bandpass DFT filter will be labeled 'IAC_Ham'.

recommended in Iacobucci and Noullez (2004, p.6). This involves applying

$$V_x(k) = (0.23 * H_{k-1} + 0.54 * H_k + 0.23 * H_{k+1}) * A_x(k). \quad (4)$$

In the above equation, $A_x(k)$ is derived from (1) and H_k is based upon the discrete ideal frequency response. The Filtering operation outlined in (3) can then be represented as

$$\tilde{y}(t_n) = \frac{1}{N}\left[\sum_{k=k_1}^{k_2} V(f_k)\exp\left(i2\pi\frac{kn}{N}\right) + \sum_{k=N-k_2}^{N-k_1} V(f_k)\exp\left(i2\pi\frac{kn}{N}\right)\right], \quad (5)$$

where $V(f_k)$ is equal to $V_x(k)$ from (4) and where $f_k = \frac{k}{N}$ is the Fourier frequency corresponding to frequency index k.

The frequency response function for the Iacobucci-Noullez filter is also displayed in Figure 1– i.e. see the 'IAC_Ham' response. The main point of difference is that the Iacobucci-Noullez filter has a smoother (tapered) transition from the stopband to passband region when compared with the conventional DFT frequency response. However, this smoothing process also allows for the possibility of increased leakage from components in the stopband to the bandpass filtered data – this would occur if components in the stopband region are very close to the 'stopband-passband' transition itself.

In Figure 2, we also display the inverse DFT to the discrete ideal Iacobucci-Noullez filter frequency response outlined in Figure 1 – i.e. see

the 'IAC_Ham' function in Figure 2. The main effect of tapering is to dampen out the filter coefficient fluctuations when compared with that associated with the conventional DFT filter.

3. SIMULATION MODEL

We wrote a FORTRAN 95 program to conduct the reported simulations. In general terms the artificial data model can be viewed as a periodic deterministic process. The 'complete' periodicity is defined as the sum of two periodicities. The first is a low frequency periodicity that is designed to fall outside the passband while the second periodicity is designed to fall within the passband.[7] Formally, define the low frequency periodicity as

$$x_l(t) = amp_1 * \sin(2\pi f_1 * (t + 10)), \tag{6}$$

and the 'bandpass' periodicity as

$$x_b(t) = amp_2 * \cos(2\pi f_2 * (t - 4)), \tag{7}$$

where amp_1 and amp_2 are amplitude parameters and f_1 and f_2 are frequency parameters. In all simulations we set $amp_1 = 5.0$ and $amp_2 = 1.0$. The complete periodicity is represented by

$$x(t) = x_l(t) + x_b(t), \tag{8}$$

[7] We adopt the same settings relating to sample size and passband that were outlined in relation to Figure 1 in the previous section.

where $x_l(t)$, $x_b(t)$ and $x(t)$ are deterministic periodic processes.

The following points should be recognized. First, the true low frequency periodicity $f_1 = 0.025$ is perfectly synchronized with the amplitude at Fourier frequency 0.025 in the low frequency region of the stopband. Second, the main difference in parameter settings adopted in (7) for the true 'bandpass' periodicity reflects our desire to examine the implications of two particular circumstances. The first corresponds to the situation where the true 'bandpass' periodicity is perfectly synchronized with a Fourier frequency amplitude in the passband (i.e. parameter $f_2 = 0.0667$). The second circumstance is where the true 'bandpass' periodicity lies between two adjacent Fourier frequency amplitudes in the passband (i.e. parameter $f_2 = 0.0625$). Plots of the artificial data series generated by (8) for both 'synchronized' and 'unsynchronized' parameter settings in (7) are documented in Figure 3.

Figure 3 about here.

The data generated by model (6)-(8) represents the 'input' series $x(t_n)$ that the time to frequency DFT in (1) is applied. The specific data series generated by (7) for f_2 parameter settings are the respective targets of the bandpass filtering operations of both types of DFT filters considered in this note.

4. SIMULATION RESULTS

Our aim is to examine the comparative performance of both DFT filters in tracking (extracting) the target data series associated with (7) from data generated by model (6)-(8) and depicted in Figure 3.

Figure 4 contains a plot of the results from application of both DFT filter algorithms to data generated by the simulation model when $f_2 = 0.0667$ in (7) (i.e. the 'synchronized' case). In this figure, the artificial data series associated with the true 'bandpass' periodicity determined by (7) (i.e. the 'actual' series) and the bandpass filtered data series from both DFT filters (i.e. the 'DFT filter' and 'IAC_Ham' series) are displayed together. It is evident from inspection of this figure that both DFT filters produce data series that perfectly track the true target periodicity – they both completely extracted the deterministic cycle corresponding to the 'true' synchronized 'bandpass' periodicity.

Figure 4 about here.

In order to confirm that the DFT filter operations have ignored the low frequency periodicity contained in (8) [generated by (6)], we plot the periodogram of the bandpass filtered data series. The periodogram is calculated as the squared modulus of the complex variable $A_x(k)$ determined from (1) for each Fourier frequency k divided by the number of sample points N. If the low frequency cycle has been removed from the filtered data series, then there should be no 'power' (i.e. no non-zero

value) at the low frequency ordinate (0.025) in the periodogram of the filtered data series. The periodograms of both DFT filtered data series are displayed in Figure 5.

Examination of Figure 5 indicates that the low frequency component has been successfully eliminated from the filtered data series – there is no power corresponding to Fourier frequency ordinate 0.025. In both cases, the only power corresponds to the spike at Fourier frequency 0.0667 reflecting the perfect synchronization with the true 'bandpass' periodicity generated by (7). Moreover, the exact correspondence between the two filtered data series can be seen by the fact that both filters display the exact same power at Fourier frequency 0.0667 in Figure 5.

Figure 5 about here.

We also investigated the ability of the two DFT filters to extract the true deterministic 'bandpass' cycle when it was not synchronized with any Fourier frequency in the passband – i.e. parameter $f_2 = 0.0625$ in (7). Note that this setting was adopted so that the 'true' periodicity falls half way between the adjacent Fourier frequencies 0.0583 and 0.0667. In Hinich, Foster and Wild (2008)b, it was demonstrated that in this case, the true periodicity would be 'smeared' or 'spread' between the adjacent Fourier frequency ordinates bordering the true periodicity.

Figure 6 contains a plot of the periodograms of the filtered data obtained from applying the DFT filters to the 'unsynchronized' data series. The first thing to note from inspection of Figure 6 is that the spike associated with the 'synchronized' case outlined in Figure 5 at Fourier frequency 0.0667 has disappeared. Instead, the true periodicity has been spread over the neighboring frequency ordinates 0.0583 and 0.0667. Moreover, there is also some power spread to other adjacent Fourier frequency ordinates in the passband region, although at a diminishing rate. It is also apparent that the pattern of dispersion about the neighboring Fourier frequency amplitudes is both qualitatively and quantitatively similar for both DFT filters. Thus, the tapering associated with the Iacobucci-Noullez filter does not affect the dispersion pattern.

Figure 6 about here.

The other major feature in Figure 6 is that the low frequency component has been successfully removed from the bandpass filtered data series – there is no power corresponding to Fourier frequency 0.025. In fact, there is no power discernible outside of the passband – all 'stopband' components have been successfully eliminated from the filtered data series.

A key question relates to the nature of possible distortions that the observed smearing of the true 'bandpass' periodicity by the DFT filters may exert on the ability of the filtered data series to replicate the true

'bandpass' periodicity. The nature of the distortions can be discerned from Figure 7 that contains plots of the DFT filtered data series against the 'unsynchronized' true 'bandpass' periodicity.

Figure 7 about here.

It is evident from Figure 7 that, apart from some noticeable deviations at both endpoints, the filtered data series seems to track the true 'bandpass' periodicity remarkably well. In fact, the main deviations apparent in Figure 7 principally reflect deviations between the true 'bandpass' periodicity and both filtered data series considered together, particularly at the endpoints.

5. CONCLUSIONS

In this note, we examined the potential impact of the Gibbs Effect upon attempts to extract a business cycle from time series data. Our objective was to examine this issue from the perspective of applied macroeconomists – namely, situations involving a single realization of a small to moderate sized samples of macroeconomic data.

We argued that the nature of the data confronting macroeconomists means that the appropriate Fourier Transform concept is the Discrete Fourier Transform. However, we also argued that the conventional theoretical results could be misleading in practice when using the DFT. Our general conclusion is that none of the problems associated with the Gibbs Effect will affect the filtering of a finite length data series using the

DFT. Essentially, the Gibbs Effect is not observable or identifiable at the frequency ordinates associated with the DFT.

In order to look at the effect of smoothing procedures to combat the Gibbs effect, we assessed the comparative performance of the conventional DFT filter with the convolved windowed DFT filter proposed by Iacobucci-Noullez. The Hamming window is utilized, using simulations involving artificial data generated from a model of a deterministic periodic process. This data was designed to contain a low frequency periodicity designed to fall outside the passband while the second periodicity was designed to fall within the passband.

The second periodicity was designed to be either synchronized with a Fourier frequency in the passband or to lie between two neighboring Fourier frequencies in the passband. In the first case, both types of DFT filters worked optimally. In the second case, however, the true periodicity was smeared between the Fourier frequencies bordering it, thus producing distortions between the true periodicity and the filtered data series, especially at the start and end points of the filtered data series.[8]

More generally, the qualitative and quantitative similarity of the results obtained for both DFT filters across the range of simulations called into

[8] It should be noted that the simulation results reported in this note can be favorably compared with the results obtained for the Baxter-King and 'bandpass' version of the Hodrick-Prescott filter reported in Hinich, Foster and Wild (2008)b, Sections 5-7. In the latter cases, the filters passed low frequency components from the 'stopband' region to the filtered data series that should not have been passed.

question the practical implications of the Gibbs Effect. If the Gibbs Effect had a significant practical role to play that was *independent* of the data generating process (as Fourier theory suggests), then we would expect the Iacobucci-Noullez filter to generate results that were different from those associated with the conventional DFT filter. This, however, did not occur.

Finally, the results cited in this note were obtained for an underlying deterministic periodic data series generated by model (6)-(8), outlined in Section 3. However, in Hinich, Foster and Wild (2008)a, Section 5, we demonstrate that our broad conclusions continue to hold when the simulation model (6)-(8) is augmented by applying the same deterministic periodic structures in (6)-(7) but augmenting (8) to include additive stationary Gaussian noise innovations.

REFERENCES

Baxter, M. and R. G. King (1999) Measuring business cycles: approximate band-pass filters for economic time series. *The Review of Economics and Statistics* 81, 575-593.

Bracewell, R. N. (1978) *The Fourier Transform and its Applications. Second Edition*. New York: McGraw-Hill.

Cogley, T. and J.M. Nason (1995) Effects of the Hodrick-Prescott filter on Trend and Difference Stationary Time Series. Implications for Business Cycle Research. *Journal of Economic Dynamics and Control* 19, 253-278.

Hinich, M. J., Foster, J. and P. Wild (2008)a Discrete Fourier Transform Filters as Business Cycle Extraction Tools: An Investigation of Cycle Extraction Properties and Applicability of 'Gibbs' Effect. *School of Economics, University of Queensland*, Discussion Paper No 357, March 2008.
(Available at: http://www.uq.edu.au/economics/abstract/357.pdf).

Hinich, M. J., Foster, J. and P. Wild (2008)b An Investigation of the Cycle Extraction Properties of Several Bandpass Filters used to Identify Business Cycles. *School of Economics, University of Queensland*, Discussion Paper No. 358, March 2008.
(Available at: http://www.uq.edu.au/economics/abstract/358.pdf).

Hodrick, R. J. and E. C. Prescott (1997) Postwar U.S. business cycles: an empirical investigation. *Journal of Money, Credit, and Banking* 29, 1-16.

Iacobucci, A. and A. Noullez (2004) A frequency selective filter for short-length time series. *OFCE Working paper N 2004-5*.
(Available at: http://repec.org/sce2004/up.4113.1077726997.pdf).

Iacobucci, A. and A. Noullez (2005) A frequency selective filter for short-length time series. *Computational Economics* 25, 75-102.

King, R.G. and S.T. Rebelo (1993) Low Frequency Filtering and Real Business Cycles. *Journal of Economic Dynamics and Control* 17, 207-231.

Kufner, A. and J. Kadlec. (1971) *Fourier Series*. Prague: Academia.

Murray, C.J. (2003) Cyclical Properties of Baxter-King Filtered Time Series. *Review of Economics and Statistics* 85, 472-476.

Papoulis, A. (1962) *The Fourier Integral and Its Applications*. New York: McGraw-Hall.

Pedersen, T.M. (2001) The Hodrick-Prescott filter, the Slutzky effect, and the distortionary effects of filters. *Journal of Economic Dynamics and Control* 25, 1081-1101.

Priestley, M. B. (1981) *Special Analysis and Time Series*. London: Academic Press.

Figure 1. Plot of Frequency Response of Selected DFT Bandpassed Filters for Unit Impulse - Sample Size = 120, Passband = (0.042,0.167)

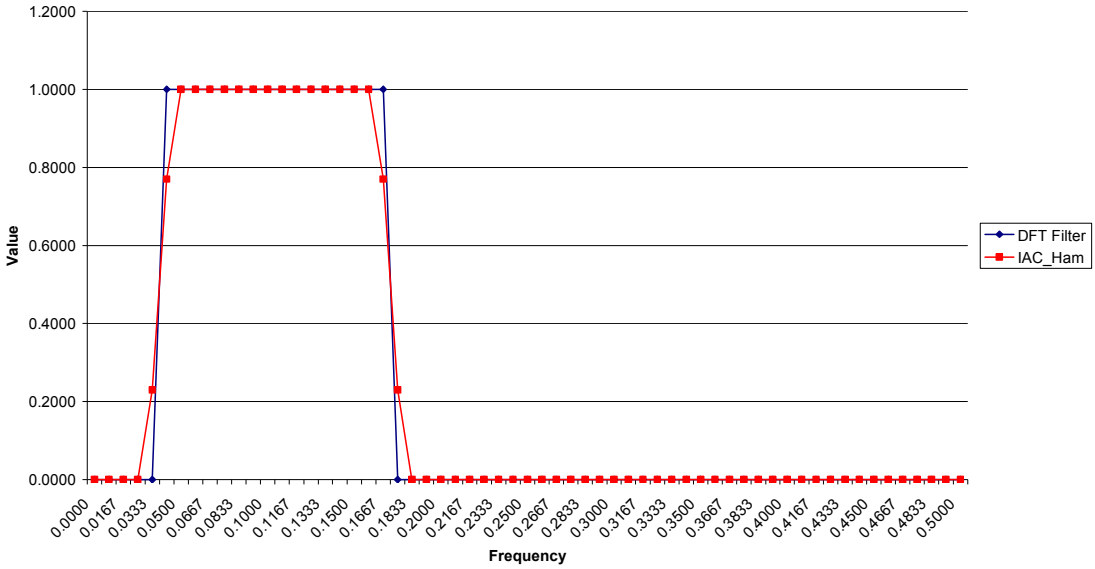

Figure 2. Plot of Inverse DFT (Dirichlet Function) of Selected DFT Bandpass Filters for Unit Impulse - Sample Size=120, Passband = (0.042,0.167)

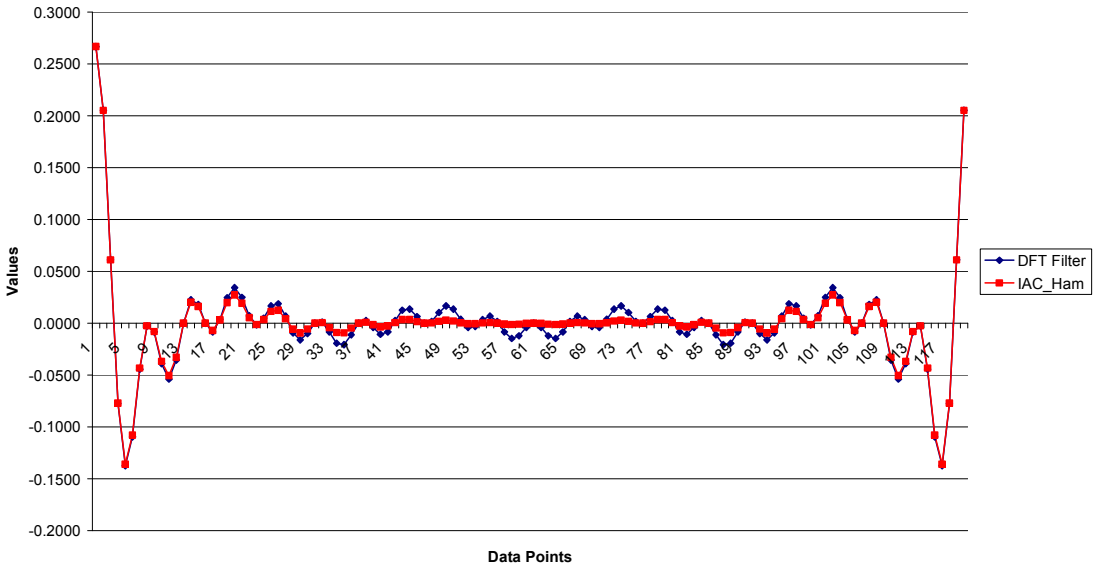

Figure 3. Plots of Complete Deterministic Periodicity [Eq (6)-Eq(8)] - Sample Size = 120, For Eq (7): f2 = 0.0625 (unsynchronized case) and f2= 0.0667 (synchronized case), respectively

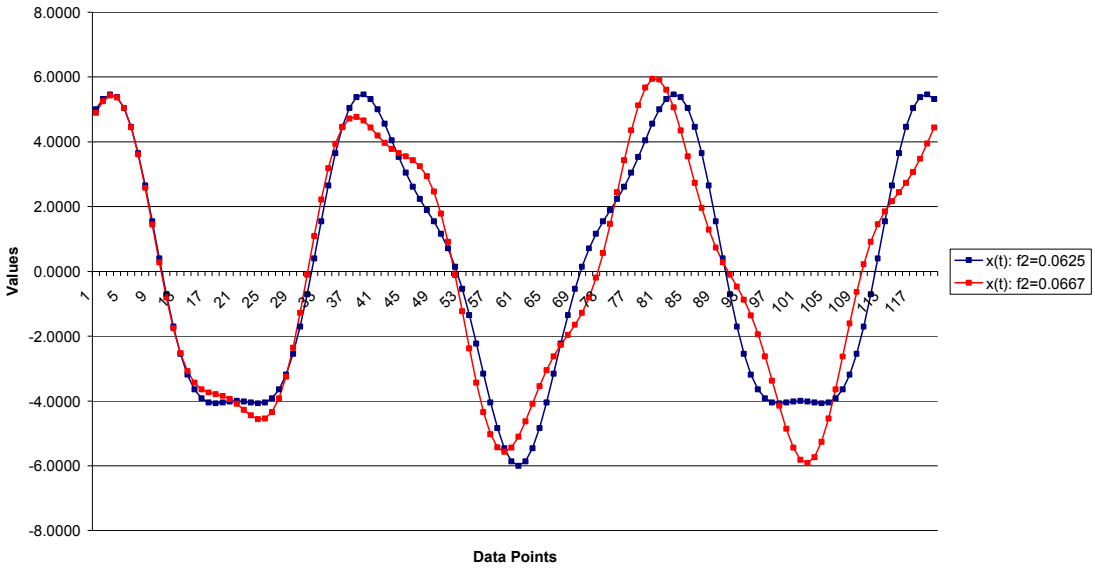

Figure 4. Comparison of DFT Filtered Data Series From Deterministic Model [Eq (6)-Eq (8)] and Actual (Target) Synchronized Bandpass Periodicity Data [Eq (7): f2 = 0.0667] - Sample Size = 120

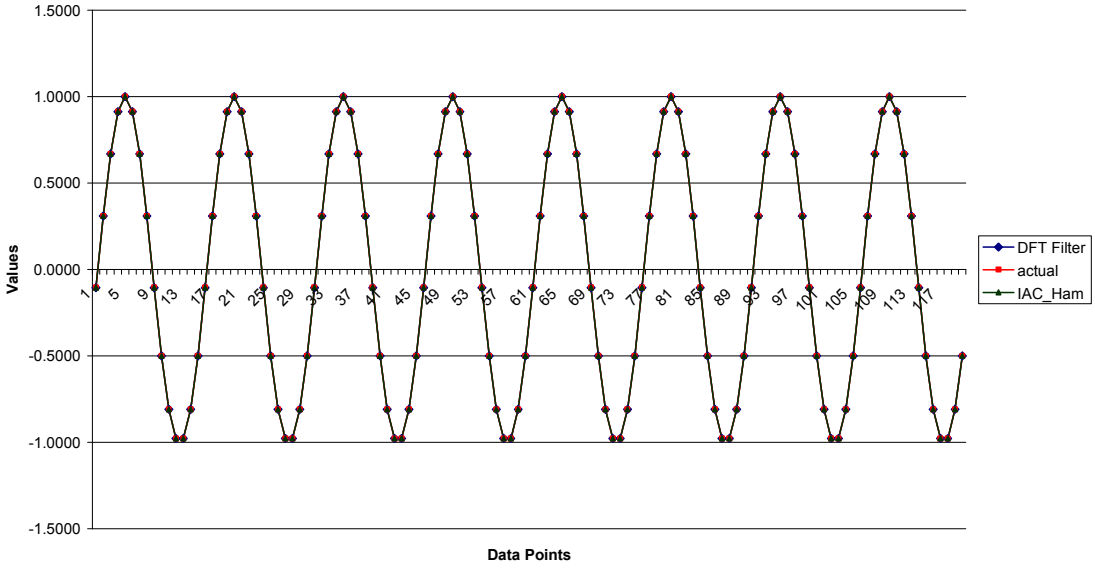

Figure 5. Plots of Periodograms of DFT Filtered Data Series Derived From Synchronized Deterministic Model [Eq (6)-Eq (8), Eq(7): f2=0.0667]: DFT and IAC_Hamming Filters - Sample Size=120, Passband = (0.042,0.167)

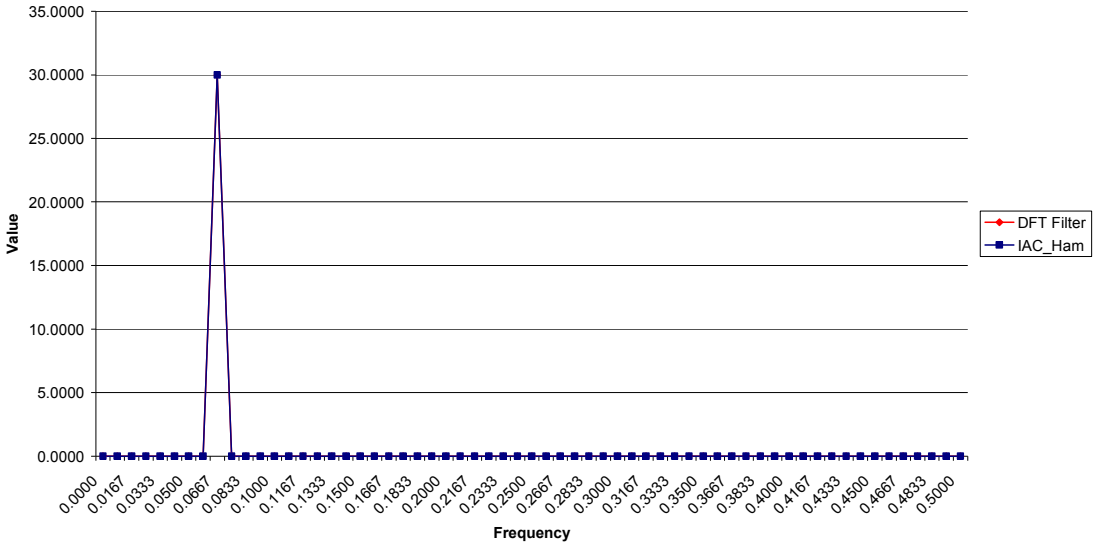

Figure 6. Plots of Periodograms of DFT Filtered Data Series Derived From Unsynchronized Deterministic Model [Eq (6)-Eq (8), Eq(7): f2=0.0625]: DFT and IAC_Hamming Filters - Sample Size=120, Passband = (0.042,0.167)

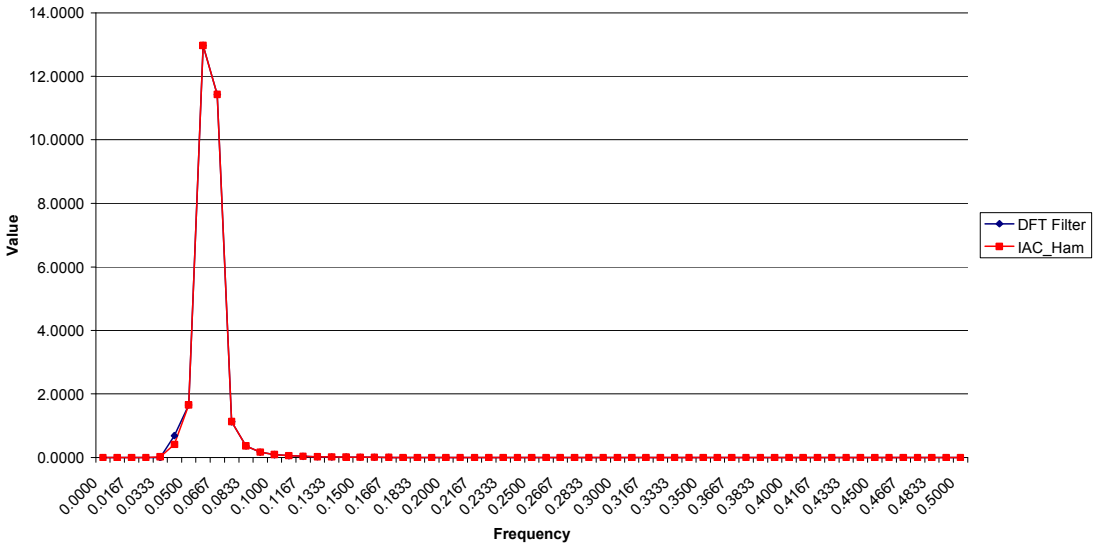

Figure 7. Comparison of DFT Filtered Data Series From Deterministic Model [Eq (6)-Eq (8)] and Actual (Target) Unsynchronized Bandpass Periodicity Data [Eq (7): f2=0.0625] - Sample Size = 120